

A 3D numerical study of solitary wave interaction with vertical cylinders using a parallelised Particle-In-Cell solver

Q. Chen^{1,*}, J. Zang¹, D. M. Kelly², A. S. Dimakopoulos³

¹Department of Architecture and Civil Engineering, University of Bath, BA2 7AY, UK

²Coastal Research Lab., International Hurricane Research Center, Florida International University, Miami FL 33199, USA

³H R Wallingford, Wallingford, Oxon, OX10 8BA, UK

*Email: chenqiang913@hotmail.com

HIGHLIGHTS

The interaction of a solitary wave with a group of eleven vertical cylinders is investigated in three spatial dimensions, using a novel parallel CFD solver that is based on the Particle-In-Cell (PIC) technique. Interesting results have been achieved for the complex scattered wave field and wave run-up on each individual cylinder within the group.

1 INTRODUCTION

Vertical cylindrical structures are widely employed in the coastal and offshore engineering area; examples include the design of oil platforms, offshore wind turbine foundations and piled wharfs. As a consequence it is important to understand the interaction of waves with multiple cylinders in terms of the free surface motion, wave run-up and wave loading in the vicinity of the structures. In the literature, numerous studies, both numerical and experimental, have been carried on this topic. For example, Mo and Liu (2009) investigated non-breaking solitary wave interaction with a single cylinder and a group of three cylinders through a Volume of Fluid (VOF) based finite volume numerical solver and also physical experiments. Kagemoto et al. (2014) carried out experimental and theoretical studies on the first-order and second-order wave interactions among an array of two rows of vertical circular cylinders. In this abstract, attention is focused on the numerical modelling of a solitary wave interacting with a group of eleven cylinders arranged in a staggered spatial configuration.

The Particle-In-Cell (PIC) based PICIN solver (Kelly et al., 2015; Chen et al., 2016) is extended to three spatial dimensions and employed for the numerical modelling. The PICIN solver is hybrid Eulerian-Lagrangian; both particles and grid are employed in this solver due to its PIC nature (see Harlow (1964)). The novelty of the PICIN model lies in the fact that the linear non-advection terms of the Navier-Stokes equations are resolved on a staggered grid (Harlow and Welch, 1965), while the nonlinear advection terms are handled using the particles in a Lagrangian manner. This makes the model both efficient and flexible in terms of simulating complex physical problems such as wave breaking and violent wave-structure interaction (see Kelly et al. (2015) and Chen et al. (2016) for more details).

2 NUMERICAL MODEL

The 3D PICIN model solves the incompressible Newtonian Navier-Stokes equations for single-

phase flow:

$$\nabla \cdot \mathbf{u} = 0, \quad (1)$$

$$\frac{\partial \mathbf{u}}{\partial t} + (\mathbf{u} \cdot \nabla) \mathbf{u} = \mathbf{f} - \frac{1}{\rho} \nabla p + \nu \nabla^2 \mathbf{u}, \quad (2)$$

where, in 3D, $\mathbf{u} = [u, v, w]^T$ is the velocity field; t is the time; p is the pressure; $\mathbf{f} = [0.0, 0.0, -9.81]^T$ represents the body force; ρ is the liquid density and ν is the kinematic viscosity of the fluid.

Both Lagrangian particles and an Eulerian grid are employed in the PICIN solver. Following Brackbill and Ruppel (1986), the particles are assigned with the mass and momentum of the fluid, while the underlying grid is solely employed for computational convenience. The overall solution is divided into two major steps: an Eulerian step and a Lagrangian step. In the Eulerian step, the Navier-Stokes equations, ignoring the advection term, are solved on the grid using the pressure projection technique, where a pressure Poisson equation is resolved incorporating the boundary conditions. For the free surface boundary, a second-order accurate technique is employed following Gibou et al. (2002), and for the solid boundary, a Cartesian cut cell based approach is utilised following Ng et al. (2009). Once the Eulerian step is completed, the divergence-free velocity field on the grid is interpolated to the particles to update the velocity field they carry. The velocity field is then advected by the particles in the Lagrangian step. Note that the velocity field on the particles is transferred back to the grid at the beginning of the Eulerian step in the next computational cycle. Interpolation schemes are used for velocity transfer between the particles and grid; in the current model, while the particle-to-grid transfer is conducted using a SPH-like kernel function, the grid-to-particle interpolation is achieved via a fourth-order accurate weighted essentially non-oscillatory (WENO) scheme. For more details of the PICIN solver, the reader is referred to Kelly et al. (2015) and Chen et al. (2016).

The current 3D PICIN model employs the state-of-the-art implementation of the open-source library OpenMPI (www.open-mpi.org) for parallelisation. In this approach the computational domain is decomposed into sub-domains based on the underlying grid and the particles are allowed to move through the sub-domains, assigning the computational loads to each process. The tests presented here were run on the High Performance Computing (HPC) system at the University of Bath, UK.

3 CASE STUDY

3.1 Numerical Setup

Figure 1 shows a sketch depicting the setup of a numerical wave tank (NWT) and the locations of a group of eleven vertical cylinders. The diameters, D , of the vertical cylinders are identical and the cylinders are symmetrically placed in the NWT, with the centre-to-centre distances being $2D$ between the adjacent cylinders in both the streamwise and the spanwise directions. The length and width of the NWT are set to $28.71D$ and $9.93D$, respectively. A piston-type wave paddle is employed at one end of the NWT as shown in Figure 1 for wave generation. The water depth, h , was fixed at $0.615D$ and the relative wave height H/h of the non-breaking solitary wave studied is 0.4. It is noteworthy that the numerical setup here is inspired by the test cases presented in Mo and Liu (2009). The grid size is set to $\Delta x = \Delta y = \Delta z = 0.04h$ and the Courant number is set to 0.5. The solitary wave is generated using the paddle wavemaker following Wu et al. (2016).

3.2 Results

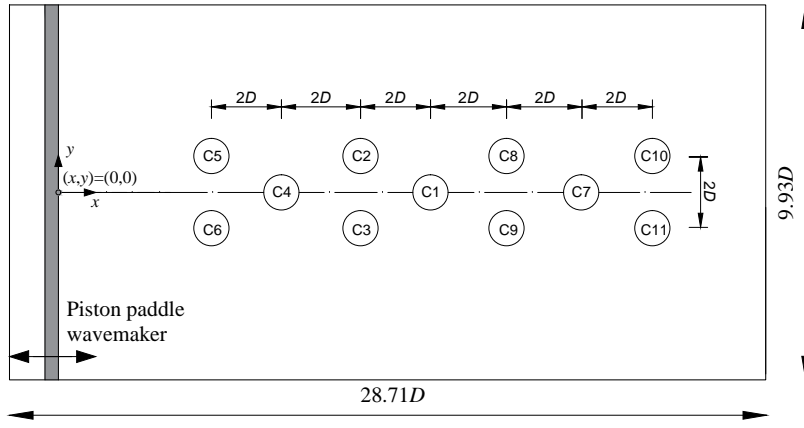


Figure 1: Sketch (top view) showing locations of the eleven cylinders in the numerical wave tank. D is the diameter of the cylinders.

Figure 2 shows two snapshots of the simulated wave field in plan view at two different time instants. The solitary wave travels from left to right. From Figure 2, it is seen that, as the solitary wave passes by the cylinders, circular scattered waves start to propagate radially in the direction away from the cylinders. Moreover, as the scattered waves interact with each other, a complex wave field forms. It can be seen from Figure 2(a) that a steep wave (maybe close to breaking) forms in front of the cylinders 5 and 6 due to the symmetric scattered waves from both cylinders interacting with each other and propagating upstream. However, as seen from Figure 2(b), similar waves emanating from cylinders 2 and 3 are blocked by cylinder 4, and the waves could be reflected back and trapped in the cylinder group 1-2-3-4.

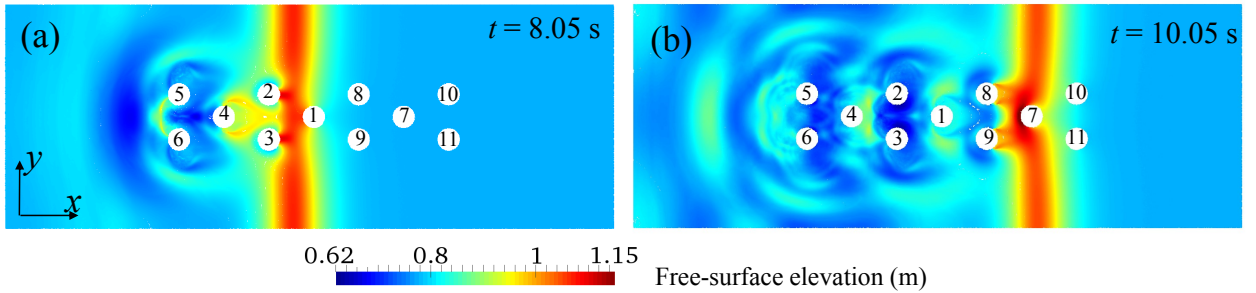


Figure 2: Snapshots (2D top view) of the numerical simulation of a solitary wave interacting with a group of eleven cylinders.

Figure 3 shows wave run-up at the upstream stagnation points of the cylinders. Since the flow field is symmetrical, the results are presented for two cylinder groups based on their positions: the first group consists of cylinders 1, 4 and 7, which are located in the middle, and the second group includes cylinders 2, 5, 8 and 10, which are located at the rightmost side, as we face downstream. The results are all shifted in time, with the time instants of all main peak values aligned with the non-dimensional time $t(g/h)^{1/2} = 0$. It can be seen that all cylinders in the first group (located in the middle) exhibit very similar wave run-up at this spatial configuration of cylinders. Similar run-up is also observed at the lateral cylinders 2, 8 and 10, with the exception of cylinder 5, which is located at the farthest front of the cylinder group. Both the first and the secondary peaks of the wave run-up at cylinder 5 appear to be the largest. In particular, the very steep secondary peak wave confirms the observations in Figure 2(a).

3 CONCLUSIONS

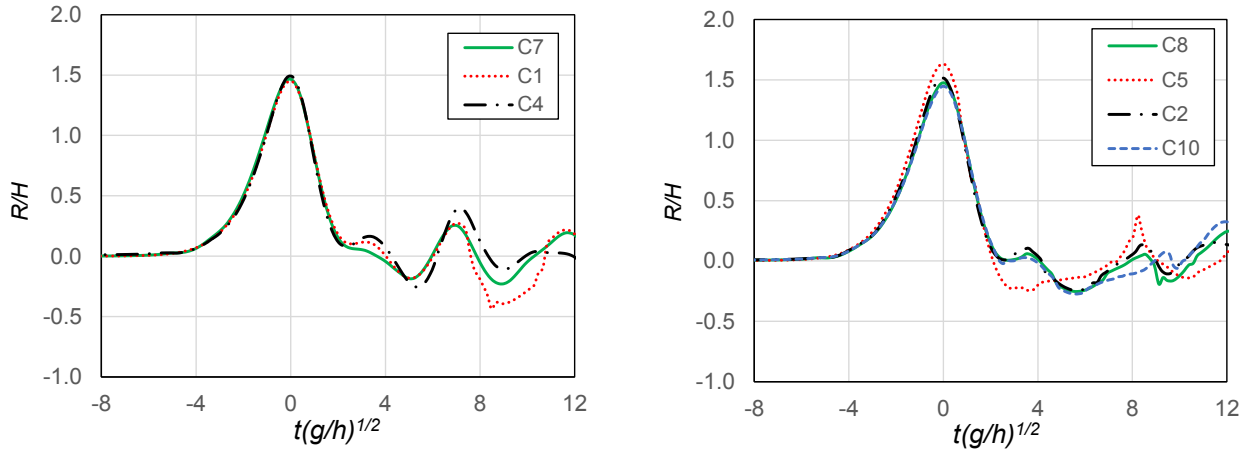


Figure 3: Comparison of wave run-up at the front stagnation points of the cylinders.

This abstract presents a numerical study of a solitary wave interacting with a group of eleven cylinders in three spatial dimensions. Complex hydrodynamic processes involving violent wave-wave and wave-structure interactions tend to occur in this case. The Particle-In-Cell based parallel PICIN solver is capable of handling such complex 3D scenarios. Additional results, including solitary wave interaction with a single cylinder and three cylinders, will also be presented.

ACKNOWLEDGEMENTS

The authors acknowledge with thanks the financial support of the University of Bath and HR Wallingford. This research made use of the Balena High Performance Computing Service at the University of Bath. DMK acknowledges the support of the IHRC at FIU.

REFERENCES

- J. U. Brackbill and H. M Ruppel. FLIP: A method for adaptively zoned, Particle-In-Cell calculations of fluid flows in two dimensions. *J. Comp. Phys.*, 65:314–343, 1986.
- Qiang Chen, Jun Zang, Aggelos S. Dimakopoulos, David M. Kelly, and Chris J.K. Williams. A Cartesian cut cell based two-way strong fluid-solid coupling algorithm for 2D floating bodies. *Journal of Fluids and Structures*, 62:252 – 271, 2016.
- Frederic Gibou, Ronald P. Fedkiw, Li-Tien Cheng, and Myungjoo Kang. A second-order-accurate symmetric discretization of the Poisson equation on irregular domains. *Journal of Computational Physics*, 176(1):205 – 227, 2002.
- F. H. Harlow. The Particle-In-Cell computing method for fluid dynamics. In B. Alder, editor, *Methods in Computational Physics*, pages 319–343. Academic Press, New York, 1964.
- F. H. Harlow and J. E. Welch. Numerical calculation of time-dependent viscous incompressible flow of fluid with free surface. *Physics of Fluids*, 8:2182–2189, 1965.
- H. Kagemoto, M. Murai, and T. Fujii. Second-order resonance among an array of two rows of vertical circular cylinders. *Applied Ocean Research*, 47:192 – 198, 2014.
- D. M. Kelly, Q. Chen, and J. Zang. PICIN: A Particle-In-Cell solver for incompressible free surface flows with two-way fluid-solid coupling. *SIAM Journal on Scientific Computing*, 37(3):B403–B424, 2015.
- Weihua Mo and Philip L.-F. Liu. Three dimensional numerical simulations for non-breaking solitary wave interacting with a group of slender vertical cylinders. *International Journal of Naval Architecture and Ocean Engineering*, 1(1):20 – 28, 2009.
- Yen Ting Ng, Chohong Min, and Frédéric Gibou. An efficient fluid–solid coupling algorithm for single–phase flows. *Journal of Computational Physics*, 228(23):8807–8829, 2009.
- Nan-Jing Wu, Shih-Chun Hsiao, Hsin-Hung Chen, and Ray-Yeng Yang. The study on solitary waves generated by a piston-type wave maker. *Ocean Engineering*, 117:114 – 129, 2016.